Performance of the IRI-2007 model for equatorial topside ion density in the African sector for low and extremely low solar activity

J. Klenzing [a,*], F. Simões [a], S. Ivanov [b], D. Bilitza [c,d], R. A. Heelis [e], and D. Rowland [a]

[a] *Space Weather Laboratory / Code 674, GSFC, Greenbelt, Maryland, USA*

[b] *Department of Physics, Georgia Institute of Technology, Atlanta, Georgia, USA*

[c] *Heliophysics Laboratory / Code 672, GSFC, Greenbelt, Maryland, USA*

[d] *Department of Physics, George Mason University, Fairfax, Virginia, USA*

[e] *Center for Space Sciences, UTD, Richardson, Texas, USA*

Abstract

The recent availability of new data sets during the recent extreme solar minimum provides an opportunity for testing the performance of the International Reference Ionosphere in historically undersampled regions. This study will present averages and variability of topside ionospheric densities over Africa as a function of season, local time, altitude, and magnetic dip latitude as measured by the Coupled Ion-Neutral Dynamics Investigation (CINDI) Mission of Opportunity on the C/NOFS satellite. The results will be compared to the three topside model options available in IRI-2007. Overall, the NeQuick model is found to have the best performance, though during the deepest part of the solar minimum all three options significantly overestimate density.

1 Introduction

The International Reference Ionosphere (IRI) is the internationally recognized model for calculating empirical ionospheric parameters such as density, composition, and temperature (Bilitza and Reinisch, 2008). IRI was founded as a joint project between the Committee on Space Research (COSPAR) and by the International Union of Radio Science (URSI). As new measurements in historically undersampled regions become available, it is important to continuously expand the underlying database for an empirical model in order to improve its utility. One such area is the African sector; recently the addition of more GPS and ionosonde stations has provided additional data (e.g., Akala et al., 2010; Bolaji et al., 2012). Additionally, it is important to look to the extremes of solar activity; during 2008 solar EUV dropped to the lowest observed values during the space age (Araujo-Pradere et al, 2011).

This paper will present topside densities as measured from the C/NOFS satellite over the African sector for periods of both low and extremely low solar activity from 2008 to 2011. Variations with respect to local time, altitude, magnetic dip latitude, and season will be compared to the predicted values from the different topside models available in IRI-2007.

2 IRI-2007

The IRI-2007 model predicts the peak density (N_mF_2) and the height (h_mF_2) of the F_2 layer based on the CCIR maps for input geophysical indices Ri_{12}, the international sunspot number (Clette et al., 2007), and IG_{12}, the

* Corresponding author
Email address: jeffrey.klenzing@nasa.gov (J. Klenzing).

"global effective sunspot number," (Liu et al., 1983). The IG_{12} index was was developed from a weighted average of ionosonde activity to estimate N_mF_2 based on the International Radio Consultative Committee (CCIR) maps of the ionosphere. However, unlike the international sunspot number, IG_{12} has no lower limit, and during the recent extreme solar minimum is often negative. Once the peak density is determined, several options may be invoked to determine the shape of the topside and bottomside profiles.

IRI-2007 includes three options for calculating topside density: the IRI-2001 model, the corrected topside model (herein referred to as IRI07-Corr), and the NeQuick model. IRI07-Corr uses a correction factor for the previous topside model as a function of altitude, dip latitude, and local time as calculated based on the topside sounder profiles from the ISIS and Alouette missions (Bilitza, 2004). The NeQuick model uses an Epstein-layer with an altitude-varying scale height (Radicella and Leitinger, 2001; Coïsson et al., 2006). This variable scale height reflects the transition of an ionosphere dominated by O^+ to one dominated by light ions at higher altitudes.

Figure 1 shows the output for the three topside options for a sample profile for the December solstice of 2010. The solid lines represent profiles at local noon; the dashed lines are at local midnight. Note that the NeQuick model diverges from the original topside model at much lower altitudes than the corrected topside profile (IRI07-Corr).

3 The C/NOFS Satellite

The C/NOFS satellite is part of a space weather mission led by the US Air Force Research Laboratory to locate, understand, and predict equatorial ionospheric scintillations (de La Beaujardière et al., 2004). The C/NOFS satellite

was launched in April 2008 into a 13° inclination orbit with perigee near 400 km and apogee near 860 km. The record-low thermospheric density during 2008 and 2009 resulted in a reduced satellite drag (Emmert et al., 2010), and the perigee and apogee of C/NOFS slowly decayed to 399 km and 810 km respectively by August 2011. The elliptical orbit allows for a sampling of ion density over multiple O^+ scale heights of the topside equatorial ionosphere. Perigee precesses through all solar local times approximately every 65 days.

C/NOFS is equipped with multiple instrument suites designed to study the ion and neutral populations and their effect on the propagation of communication signals. Of interest to this study is the ion density (electron density for a quasi-neutral plasma), which is provided by the Retarding Potential Analyzer (RPA) from the Coupled Ion-Neutral Dynamics Investigation (CINDI) suite of instruments. The RPA technique is a well-established *in situ* method of sampling ion density, temperature, and composition (Heelis and Hanson, 1998).

Sample CINDI data is shown in Figure 2, along with the IRI-2007 predictions using the three topside options. Panel (a) shows three orbits from 4 Nov 2010 (when perigee is at local noon); panel (b) shows the same for 6 Dec 2010 (when perigee is at local midnight). In each case, perigee is marked by the vertical dashed blue line. Because the perigee of C/NOFS is near 400 km, the various bottomside options will not be investigated in this study. By averaging both the measured and predicted values over all orbits for a sufficient number of days, the performance of IRI can be investigated as a function of local time, altitude, and geographic position.

4 Statistical performance of the topside options for IRI-2007

For this study, the data will be broken into four seasons per year according to Table 1. Each season will consist of 91 days centered about the appropriate solstice/equinox, and the two equinoctial seasons remain separate. Summary plots from the March equinox of 2011 are not included in this study because the rapidly change solar flux makes it difficult to reconstruct the average ionosphere over a 91-day period. Predicted densities from the three topside models are calculated every five seconds along every orbit, and the same averaging techniques applied to the data are also applied to the modeled values before comparison. Data beyond August 2011 will not be considered, as the definitive values of Ri_{12} and IG_{12} beyond this month have not been released at the time of this paper. While the average values of Ri_{12} and IG_{12} are reported in Table 1 for each 91-day season, the actual monthly values were used to run IRI-2007.

The averaging techniques used here are similar to those applied in Klenzing et al. (2011). In summary, a Savitsky-Golay filter (Savitsky and Golay, 1964) is used on the CINDI data to remove small-scale irregularities, and only geomagnetically quiet times where K_p is less than 3 for the preceding 24 hours are used in the averages. For this study, we will only consider geographic longitudes in the African sector (between 20° W and 60° E). The data will be averaged over local time (with a bin width of 2.5 hours), altitude (50 km), and dip latitude (5 degrees). The orbit of the satellite does not allow for a complete coverage over all three dimensions, so certain slices through the three-dimensional space have been chosen to maximize the information conveyed.

The data will be presented as mean values with a standard deviation. This reflects the day-to-day variability of the ionosphere, even under geomagnet-

ically quiet times. It is important to remember that IRI provides monthly averages of data. Previous studies have shown that there is a significant variation of the peak density in the African sector, particularly near the dawn terminator (Akala et al., 2010). A concurrent study by Simões et al. (2012) of the Ionospheric Alfvén Resonator (IAR) over Africa found that both the mean CINDI averages used in this study and the IRI predicted density profile produced a similarly large error when modeling the spectral response of an assumed density profile. However, there was a significant improvement in the IAR model when the mean density minus one standard deviation was used instead, indicating that the day-to-day variability is important when considering individual profiles.

4.1 Variation with Local Time

Figure 3 shows the performance of the three topside models in the African sector near 12° S dip latitude for the solstitial periods under consideration. This latitude was chosen because it has the most complete coverage over local time due to the orbital precession. For each season, the average ion density between 400 and 450 km is plotted as a black line, with the error bars representing standard deviation. The results from the three models are plotted as dashed lines. Note that at these altitudes, there is vey little difference between the IRI-2001 topside model and the corrected topside model. Through the June solstice of 2010, all three topside models are high by more than one standard deviation for most of the day. For the December solstice of 2010 and June solstice of 2011, the IRI estimates are with one standard deviation of the mean density. In all cases, the NeQuick model performs slightly better than the other two options.

Figure 4 shows the performance for altitudes between 760 and 810 km

(near the C/NOFS apogee) for the same six seasons. For these altitudes, the three topside models produce significantly different predicted densities. For all seasons, the NeQuick model has the best performance, outperforming the IRI-2001 and IRI07-Corr models by a factor of 3 and 2, respectively. Note that there is still a significant overestimate (>2 standard deviations) during much of the daytime June solstices.

Figure 5 shows the performance near perigee for the four equinoctial seasons. Note that not all local times for the March equinox of 2010 are available. In general, the NeQuick model has the best performance at this altitude. There are several notable exceptions to this (such as the post-sunset hours for March 2010), but for these times all three models fall within one standard deviation of the the average density data. During the September equinox of 2010, the NeQuick estimates at nearly all local times fall within one standard deviation of the data; only the local times near dawn shown an overestimate.

The densities for the equinoctial seasons near apogee (760 to 810 km) are shown in Figure 6. As in Figure 4, the three topside models predict significantly different densities. NeQuick performs significantly better than the other two options, but still overestimates by more than one standard deviation during the day in 2009.

4.2 Variation with Dip Latitude

The variation of the afternoon ion density with respect to magnetic dip latitude is shown in Figure 7. Only data near perigee (400 to 450 km) will be used for the dip latitude plots in order to have the best opportunity to observe the southern Equatorial Ionization Anomaly (EIA) crest in the CINDI data. In all cases, NeQuick provides a slight advantage in calculating the density. There

is little difference between the IRI-2001 and IRI07-Corr models for this region. For December 2008 (Figure 7a), the EIA crest appears in the data about 4° of magnetic latitude north of its predicted location by IRI. By December 2010 (7e), the EIA crest appears in the data at or near its predicted location.

The anomaly crest near midnight is shown in Figure 8 for the same six seasons. Note that for nighttime, there is a greater divergence between the IRI-2001 and the corrected topside models for dip latitudes greater than 6° S. NeQuick provides the best estimate of the three options; it performs particularly well for the southern half of the two equinoctial plots. For June 2010, the EIA crest appears about 3 degrees north of its predicted location at midnight.

Figure 9 shows the afternoon position of the southern EIA crest for the periods of extremely low solar activity. Note that the position of the anomaly crest is unclear in all but September 2010 (9d). The nighttime plots with respect to dip latitude are shown in Figure 10.

5 Discussion

For all seasons and solar activities, the NeQuick topside option performs best when compared to average in situ measurements of ion density. This is consistent with previous studies of vTEC over Africa (Adewale et al., 2012), as well as topside sounder data from the ISIS and Alouette missions (Bilitza, 2009). Additionally, the NeQuick model represents a significant improvement over the other options at high altitudes. Indeed, the performance at the higher altitudes is likely to be the cause of the discrepancy previously reported in vTEC measurements (Adewale et al., 2012). Note that there are some seasons where NeQuick is more likely to overestimate at higher altitudes (in particular, the June solstice), indicating that the model does not decrease with altitude

as rapidly as it should.

There tends to be an overestimate near the dawnside terminator between 4 and 8 SLT for altitudes near the F-peak, which goes away for higher altitudes. This is consistent with observations from GPS vTEC over Africa (Adewale et al., 2012) and observations from CHAMP in the equatorial region (Lee et al., 2011).

During the recent solar minimum between cycles 23 and 24, solar EUV flux dropped to record low levels, well below what would have been expected based on observations of F10.7 (Chen et al., 2011). This was confirmed not only from direct measurements of EUV (Araujo-Pradere et al, 2011), but also through the demonstration that the neutral atmosphere was contracted beyond expectation through satellite drag calculations (Solomon et al., 2010) and direct measurement of the neutral scale height (Haaser et al., 2010). Ionospheric behavior during the extreme solar minimum was more complicated than that of the neutrals because the response to EUV changes is non-linear (Araujo-Pradere et al, 2011). The vertical $\mathbf{E}\times\mathbf{B}$ drifts were found to be significantly different, including the absence of the pre-reversal enhancement during 2008 and 2009 and downward drifts during the early afternoon (Pfaff et al., 2010; Stoneback et al., 2011).

Previous studies utilizing the CHAMP and GRACE satellites have shown that IRI-2007 topside overestimation occurs as early as 2006 (Lühr et al., 2010; Lee et al., 2011); this study along with the global equatorial averages presented in Klenzing et al. (2011) shows that as solar cycle 24 proceeds, the performance of the IRI model − specifically, NeQuick − improves significantly.

The EIA density crest, sometimes referred to as the Appleton anomaly, is a result of the equatorial fountain effect, where plasma near the magnetic

equator is lifted up by $\mathbf{E}\times\mathbf{B}$ drifts and slowly diffuses down the field lines (e.g., Schunk and Nagy, 2000). During December of 2008, the EIA crest as observed in the CINDI data appears about four degrees closer to the magnetic equator than predicted. This discrepancy is likely to be an effect of the contracted ionosphere, and may be the result of the anomaly crest moving down in altitude, moving in to neighboring flux tubes, or a combination of both.

6 Summary

The performance of the three topside model options of the International Reference Ionosphere (IRI) were compared to *in situ* measurements of density from the C/NOFS satellite in the African sector (20° W to 60° E) for periods of low and extremely low solar activities. The major findings were:

(1) The NeQuick topside model performs the best overall when compared to the mean *in situ* data. The only exceptions to this observation occur when all three models are within one standard deviation of the mean.

(2) At higher altitudes (∼800 km), there is a significant overestimate of density by the IRI-2001 and IRI07-Corr topside models for all seasons compared.

(3) During the extreme solar minimum of 2008 and 2009, all topside options tend to overestimate density in the topside ionosphere over Africa.

(4) The southern EIA crest over Africa is about 4 degrees closer to the magnetic dip equator than predicted by IRI during the December solstice of 2008.

(5) The performance of IRI in the summer hemisphere is dramatically improved during 2010. IRI still tends to overestimate electron density during the winter for dip latitudes greater than 15 degrees.

Acknowledgments

The work performed by JK and FS is supported by appointment to the NASA Postdoctoral Program at Goddard Space Flight Center, administered by Oak Ridge Associated Universities through a contract with NASA. The work performed by SI at Goddard Space Flight Center was made possible by the NASA Education Office through the Undergraduate Student Research Program managed by the Universities Space Research Association. DB is supported through NASA grant NNX09AJ74G S04. The work at the University of Texas at Dallas is supported by NASA grant NAS5-01068 and NASA grant NNX10AM94G. F10.7, Ri_{12}, and IG_{12} are provided by the UK World Data Center, and K_p is provided through CDAWeb/GSFC.

References

Adewale, A.O., Oyeyemi, E.O., Cilliers, P.J., McKinnell, L.A., Adeloye, A.B. Low solar activity variability and IRI 2007 predictability of equatorial Africa GPS TEC, Adv. Space Res., 49, 316-326, 2012.

Akala, A.O., Oyeyemi, E.O., Somoye, E.O., Adeloye, A.B., Adewale, A.O. Variability of foF2 in the African equatorial ionosphere, Adv. Space Res., 45, 1311-1314, 2010.

Araujo-Pradere, E.A., Redmon, R., Fedrizzi, M., Viereck, R., Fuller-Rowell, T.J. Some Characteristics of the Ionospheric Behavior During the Solar Cycle 2324 Minimum, Solar Phys., DOI 10.1007/s11207-011-9728-3, 2011.

Bilitza, D. A correction for the IRI topside electron density model based on Alouette/ISIS topside sounder data. Adv. Space Res. 33 (6), 838 843, 2004.

Bilitza, D., Reinisch, B.W., Radicella, S.M., Pulinets, S., Gulyaeva, T., Triskova, L., Improvements of the International Reference Ionosphere

model for the topside electron density profile, Radio Sci., 41, RS5S15, doi:10.1029/2005RS003370, 2006.

Bilitza, D., Reinisch, B.W. International Reference Ionosphere 2007: Improvements and new parameters, Adv. Space Res., 43, 599, doi:10.1016/j.asr.2007.07.048, 2008.

Bilitza, D. Evaluation of the IRI-2007 model options for the topside electron density, Adv. Space Res., 44, 701, doi:10.1016/j.asr.2009.04.036, 2009.

Bolaji, O.S., Adeniyi, J.O., Radicella, S.M., Doherty, P.H. Variability of total electron content over an equatorial West African station during low solar activity, Radio Sci., 47, RS1001, doi:10.1029/2011RS004812, 2012.

Chen, Y., Liu, L., Wan, W. Does the $F_{10.7}$ index correctly describe the solar EUV flux during the deep solar minimum of 2007-2009?, J. Geophys. Res., 116, A04304, doi:10.1029/2010JA016301, 2011.

Clette, F., D. Berghmans, P. Vanlommel, R. A. M. Van der Linden, A. Koeckelenbergh, and L. Wauters, From the Wolf number to the International Sunspot Index: 25 years of SIDC, Adv. Space Res., 40, 919-928, doi:10.1016/j.asr.2006.12.045, 2007.

Coïsson, P., Radicella, S.M., Leitinger, R., Nava, B. Topside electron density in IRI and NeQuick: features and limitations. Adv. Space Res. 37 (5), 2006.

de La Beaujardière, O. and the C/NOFS Definition Team, C/NOFS: a mission to forecast scintillations, J. Atmos. and Sol-Terr. Phys,, 66, 1573, doi:10.1016/j.jastp.2004.07.030, 2004.

Emmert, J.T., Lean, J.L., Picone, J.M. Record-low thermospheric density during the 2008 solar minimum, Geophys. Res. Lett., 37, L12102, doi:10.1029/2010GL043671, 2010.

Haaser, R.A., Earle, G.D., Heelis, R.A., Coley, W.R., Klenzing, J. H. Low-latitude measurements of neutral thermospheric helium dominance near 400 km during extreme solar minimum, J. Geophys. Res., 115, A11318, doi:10.1029/2010JA015325, 2010.

Heelis, R.A., Hanson, W. B. "Measurements of thermal ion drift velocity and temperature using planar sensors," in *Measurement Techniques in Space Plasmas (Geophys. Monogr. Ser. vol. 102)*, edited by R. F. Pfaff, J. E. Borovsky, and D. T. Young, (AGU, Washington, D. C., 1998) p. 61.

Klenzing, J., Simões, F., Ivanov, S., Heelis, R.A., Bilitza, D., Pfaff, R., Rowland, D. Topside equatorial ionospheric density and composition during and after extreme solar minimum, J. Geophys. Res., 116, A12330, doi:10.1029/2011JA017213, 2011.

Lee, C.-K., Han, S.-C, Bilitza, D., Chung, J.-K., Validation of international reference ionosphere models using in situ measurements from GRACE K-band ranging system and CHAMP planar Langmuir probe J Geod, 85, 921929 doi:10.1007/s00190-011-0442-6, 2011.

Liu, R. Y., P. A. Smith, and J. W. King, A new solar index which leads to improved foF2 predictions using the CCIR Atlas, Telecomm. J., 50, 408-414, 1983.

Lühr, H., Xiong, C. IRI-2007 model overestimates electron density during the 23/24 solar minimum, Geophys. Res. Lett., 37, L23010, doi:10.1029/2010GL045430, 2010.

Pfaff, R., Rowland, D., Freudenreich, H., Bromund, K., Le, G., Acuña, M., Klenzing, J., Liebrecht, C., Martin, S., Burke, W.J., Maynard, N.C., Hunton, D.E., Roddy, P.A., Ballenthin, J.O., Wilson, G.R., Observations of DC Electric Fields in the Low Latitude Ionosphere and Their Variations with Local Time, Longitude, and Plasma Density during Extreme Solar Minimum, *J. Geophys. Res., 115,* A12324, doi:10.1029/2010JA016023, 2010.

Radicella, S.M., Leitinger, R. The evolution of the DGR approach to model electron density profiles. Adv. Space Res. 27, 3540, 2001.

Russell, C.T., Luhmann, J.G. Jian, L.K. How unprecedented a solar minimum?, Rev. Geophys., 48, RG2004, doi:10.1029/2009RG000316, 2010.

Savitzky, A., and M. J. E. Golay, Smoothing and differentiation of data by

simplified least squares procedures, *Anal. Chem., 36*, 1627-1639, 1964.

Schunk, R.W., Nagy, A.F., Ionospheres: Physics, Plamsa Physics, and Chemistry, Cambridge University Press, Cambridge, UK, 2000.

Simões, F., Klenzing, J., Ivanov, S., Pfaff, R., Freudenreich, H., Bilitza, D., Rowland, D., Bromund, K., Liebrecht, M.C., Martin, S., Schuck, P., Uribe, P., Yokoyama, T., Detection of ionospheric Alfvén resonator signatures in the equatorial ionosphere, J Geophys. Res. - Space Physics (under review), 2012.

Solomon, S.C., Woods, T.N., Didkovsky, L.V., Emmert, J.T., Qian, L. Anomalously low solar extreme-ultraviolet irradiance and thermospheric density during solar minimum, Geophys. Res. Lett., 37, L16103, doi:10.1029/2010GL044468, 2010.

Stoneback, R.A., Heelis, R.A., Burrell, A.G., Coley, W.R., Fejer, B.G., E. Pacheco, E. Observations of quiet time vertical ion drift in the equatorial ionosphere during the solar minimum period of 2009, J. Geophys. Res., 116, A12327, doi:10.1029/2011JA016712, 2011.

Table 1

Seasonal divisions for the topside profile reconstructions, including the average solar activity represented by F10.7, Ri_{12}, and IG_{12} for each period.

Period	Range of Days	F10.7	$\sigma_{F10.7}$	Ri_{12}	IG_{12}
Dec Solstice 2008	6 Nov 2008 – 4 Feb 2009	67.2	0.9	2.0	-9.2
Mar Equinox 2009	3 Feb 2009 – 4 May 2009	69.1	1.2	2.0	-8.4
Jun Solstice 2009	7 May 2009 – 5 Aug 2009	70.1	2.0	3.2	-6.3
Sep Equinox 2009	8 Aug 2009 – 6 Nov 2009	70.7	2.5	6.2	-0.8
Dec Solstice 2009	6 Nov 2009 – 4 Feb 2010	75.1	4.7	8.5	3.9
Mar Equinox 2010	3 Feb 2010 – 4 May 2010	80.8	5.0	12.6	10.4
Jun Solstice 2010	7 May 2010 – 5 Aug 2010	77.7	5.4	16.8	15.7
Sep Equinox 2010	8 Aug 2010 – 6 Nov 2010	81.2	4.4	21.1	19.1
Dec Solstice 2010	6 Nov 2010 – 4 Feb 2011	81.1	4.2	29.4	26.2
Jun Solstice 2011	7 May 2011 – 5 Aug 2011	98.8	10.6	53.4	56.1

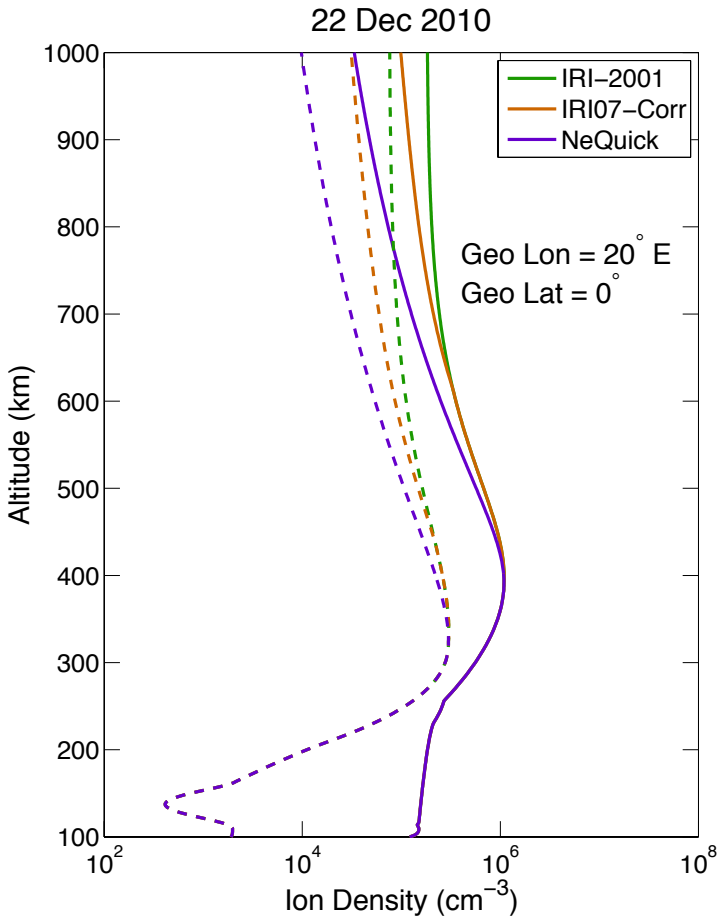

Fig. 1. Sample IRI-2007 profiles, illustrating the differences between the three topside models. Density profiles at local noon are solid lines; profiles at local midnight are dashed.

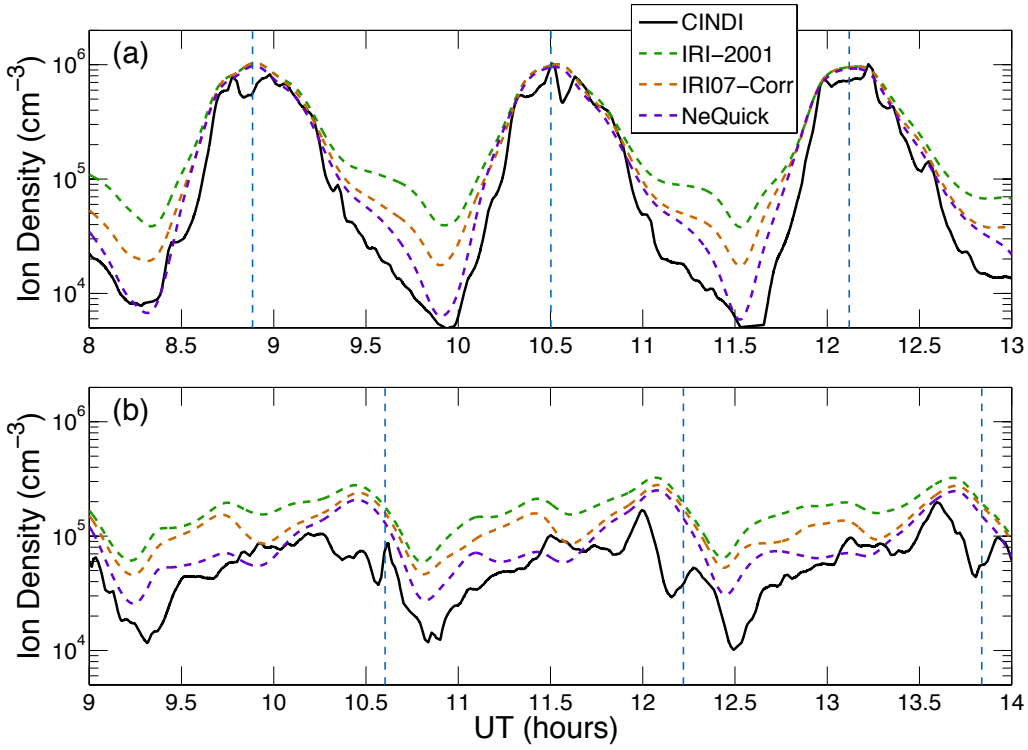

Fig. 2. Sample CINDI data for three consecutive orbits, compared with the IRI predicted densities for each topside model. The vertical dashed lines represent perigee ($\sim$ 400km).

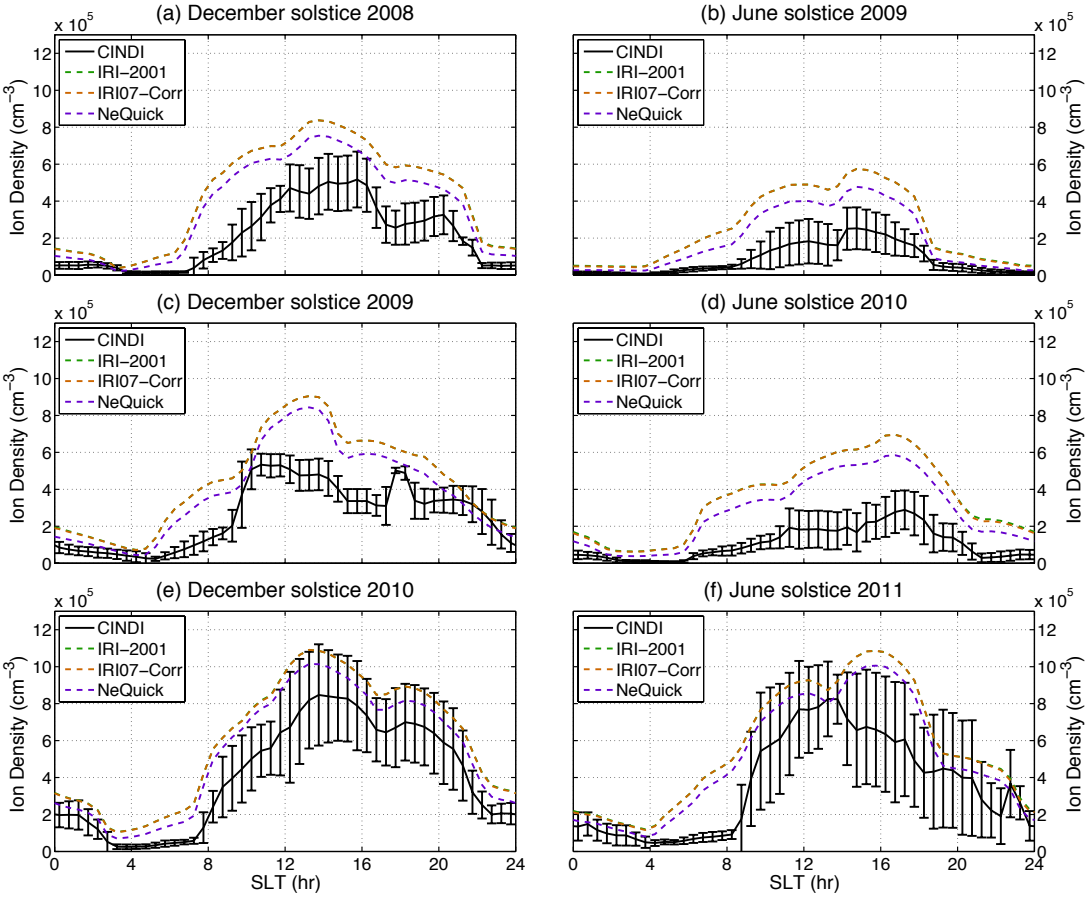

Fig. 3. Comparison of the three topside options of IRI for ion density with the CINDI data for a period of low solar activity. The data is averaged between 400 and 450 km altitude at 12° S magnetic dip latitude. Note that the IRI-2001 and the IRI07-Corr models significantly overlap at these altitudes.

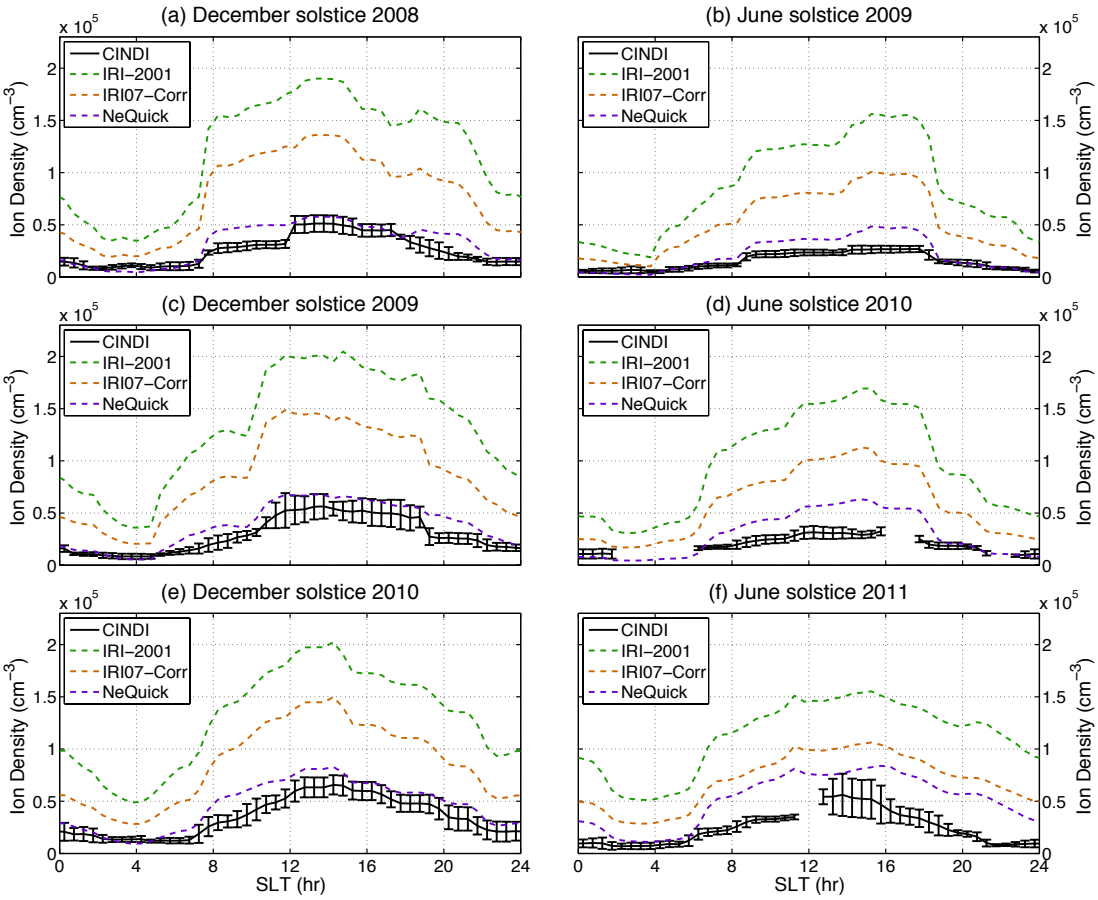

Fig. 4. The same as Figure 3, but for altitudes between 760 and 810 km,

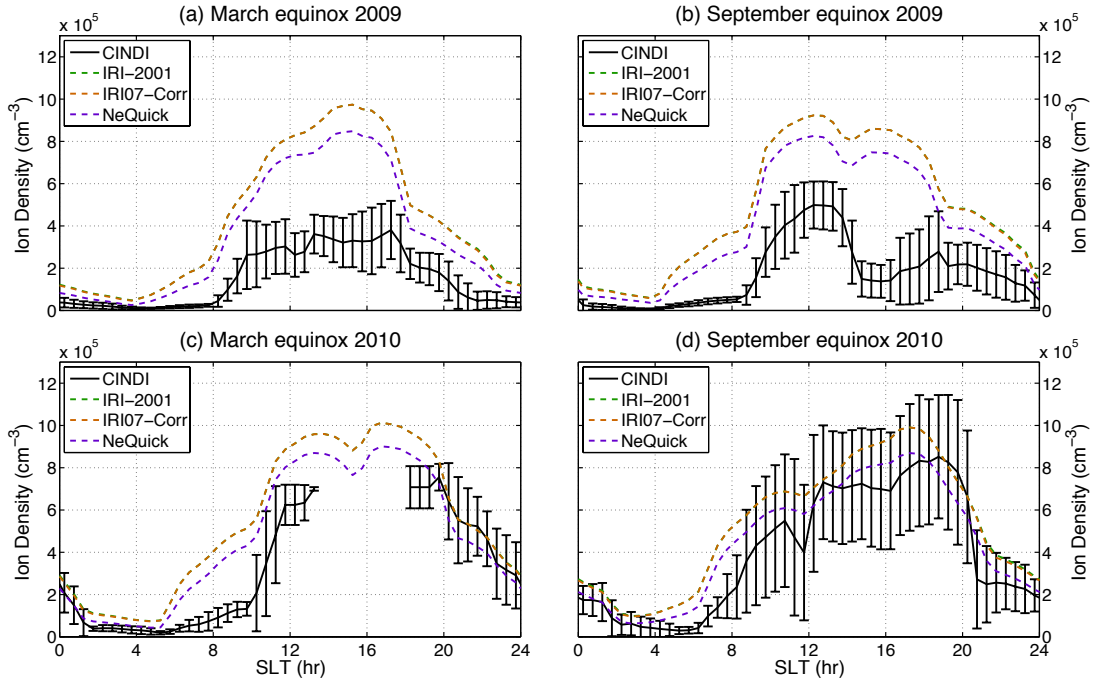

Fig. 5. The same as Figure 3, but for the equinoctial seasons.

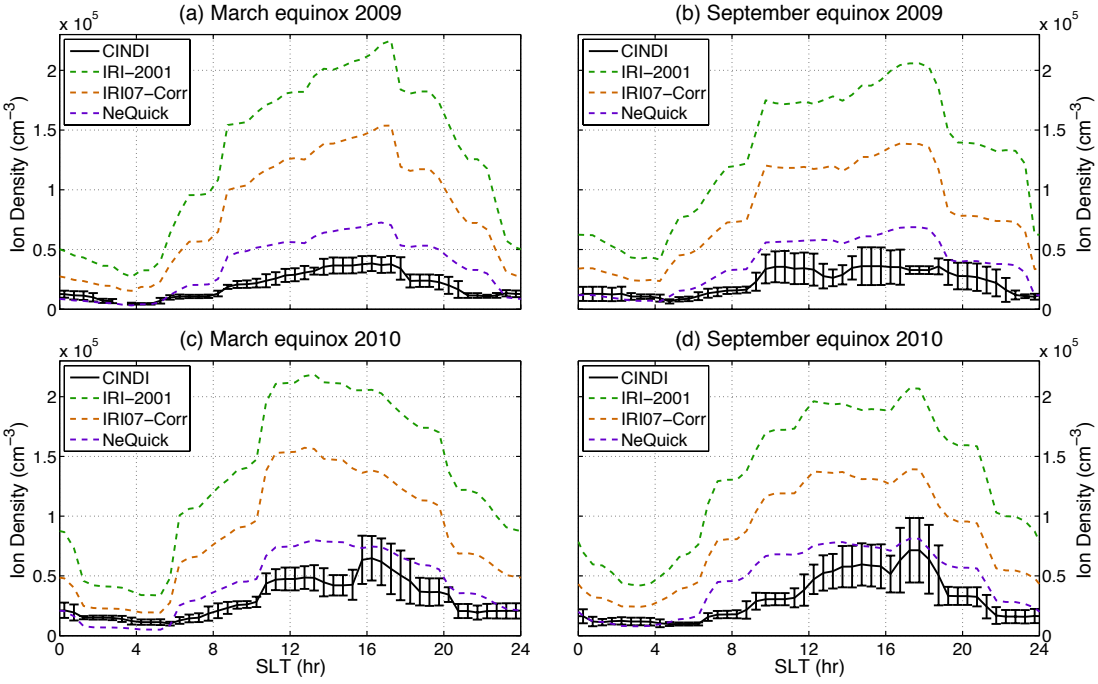

Fig. 6. The same as Figure 4, but for the equinoctial seasons.

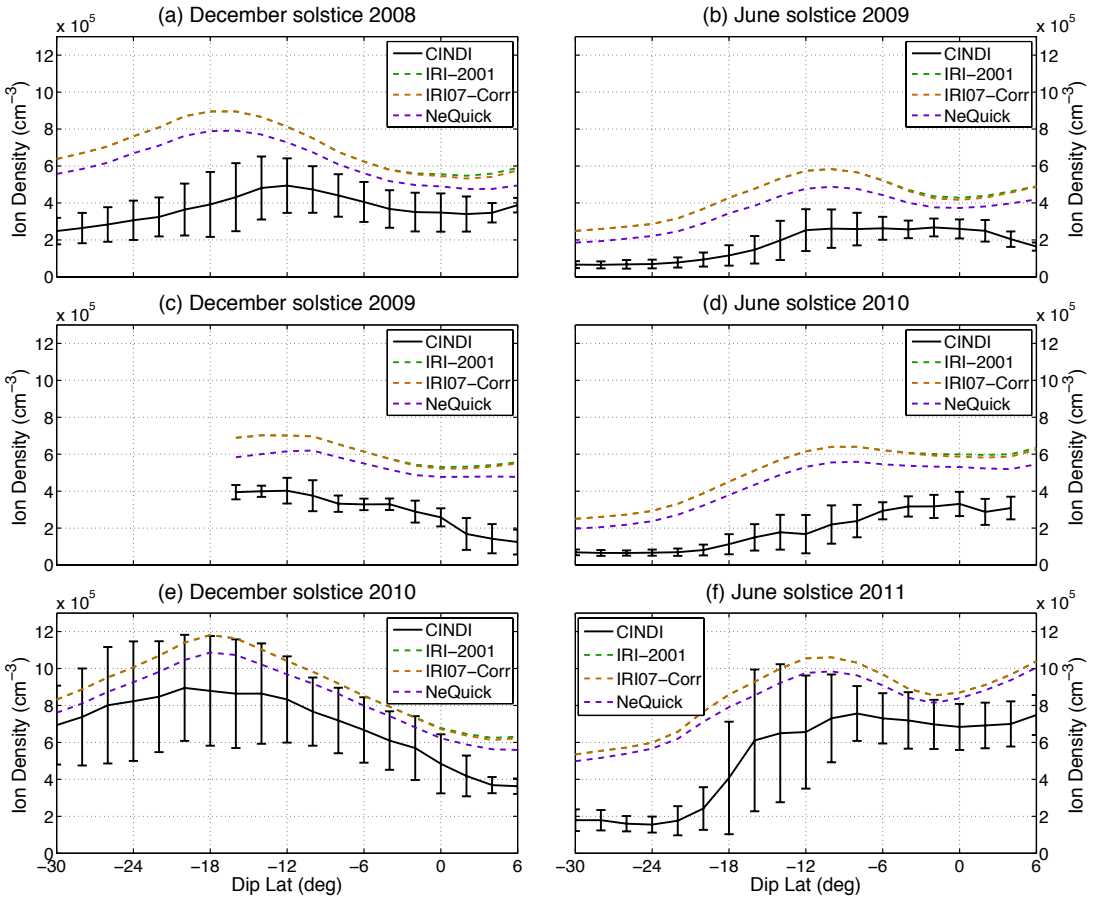

Fig. 7. Comparison of the three topside options of IRI for ion density with the CINDI data for a period of low solar activity. The data is averaged between 400 and 450 km altitude and between 13.5 and 16 hours of solar local time.

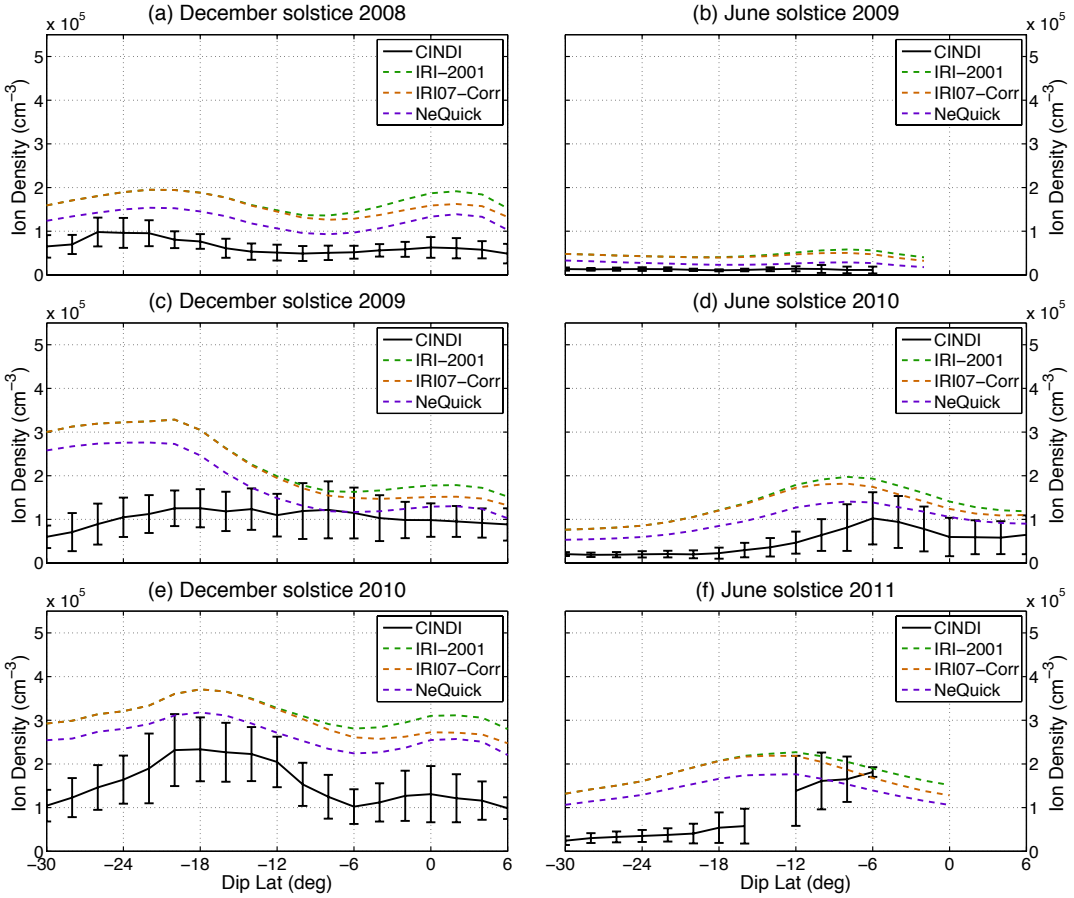

Fig. 8. The same as Figure 7, but near local midnight. Data is averaged between 22.5 and 1 hours of solar local time.

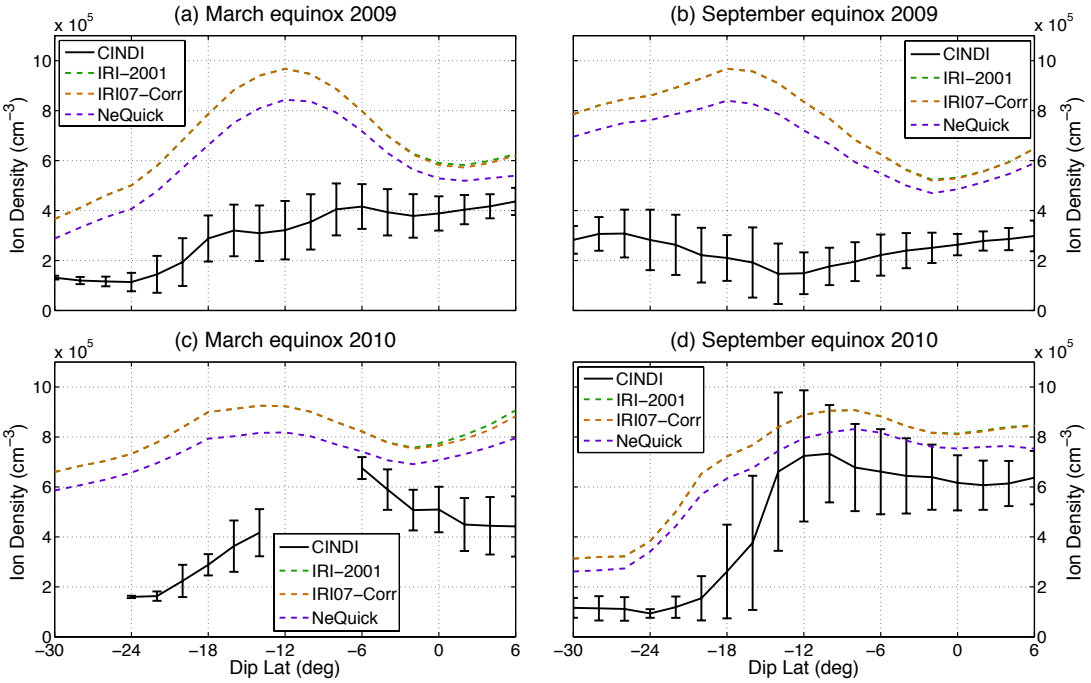

Fig. 9. The same as Figure 7, but for the equinoctial seasons.

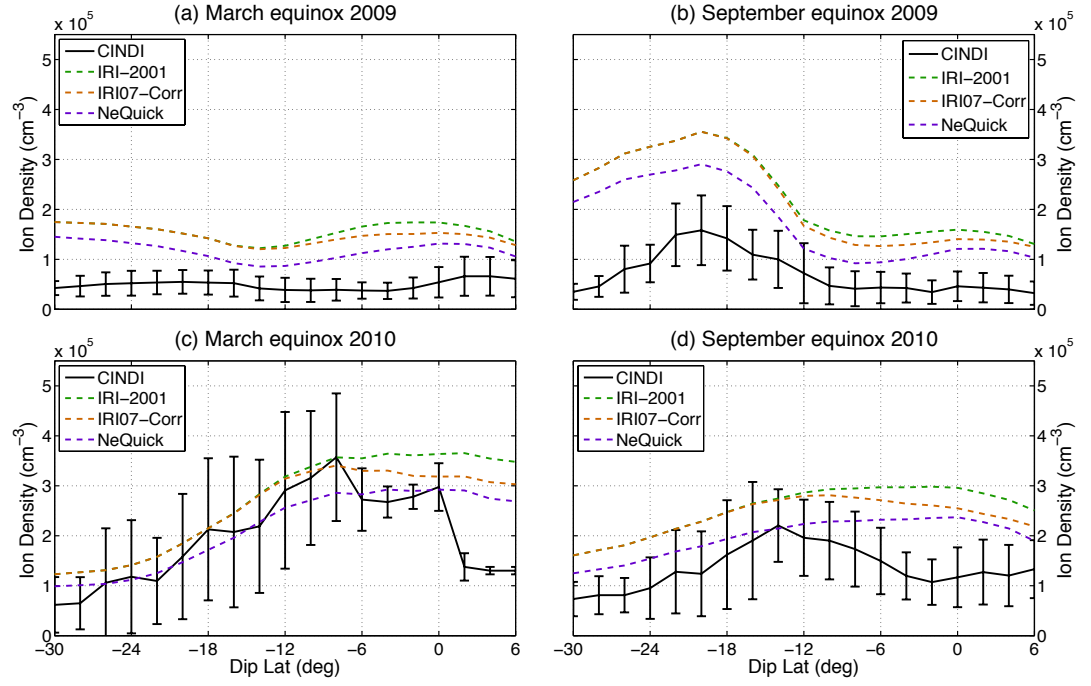

Fig. 10. The same as Figure 8, but for the equinoctial seasons.